NONLINEAR ANALYSIS OF FREE FLIGHT ROCKETS USING MSC/NASTRAN

By: David S. Livshits*, TAAS - Israel Industries Ltd.
David Saltoun** , MSI, Israel

ABSTRACT

A finite element model for nonlinear dynamic analysis of a free flight rocket is developed in this paper. The rocket response time history is calculated as a result of aerodynamic loads, dynamic imbalance and thrust misalignment. The aerodynamic loads are calculated using combinations of NOLINs. The model can perform aeroelastic stability analysis and loads distribution calculations as a function of time. A nonlinear aerodynamic behavior can be included in the model for large angles of attack.

(*) - Senior Dynamics Specialist
(**) - Manager

Nomenclature

L_N - lift force on a rocket nose
L_T - lift force on a rocket tail
V - rocket velocity
ρ – air density
$C_{L_\alpha}^N$ - lift force coefficient on a rocket nose
$C_{L_\alpha}^T$ - lift force coefficient on a rocket tail
A - reference area
α_N - nose angle of attack
α_T - tail angle of attack
q - rocket pitch velocity
x_N - distance between the nose aerodynamic center and the rocket center of mass
x_T - distance between the tail aerodynamic center and the rocket center of mass
T - thrust force
T_L - lateral thrust component caused by the thrust misalignment
[M] - rocket mass matrix
[C] - rocket damping matrix
[K] - rocket stiffness matrix
$\{F(t,x,\dot{x})\}$ - forcing functions vector
x_a - rocket aerodynamic center coordinate measured from the tail
$x_{c.g.}$ - rocket center of gravity coordinate measured from the tail
S.M. - stability margin
ω - rocket spin
z_m - eccentric mass distance from the rocket axis
g - gravity acceleration
α_m - thrust misalignment angle
α_d - dynamic imbalance angle
I_{xx} - rocket rolling moment of inertia
I_{zz} - rocket rolling moment of inertia

Introduction

The research presented herein has been initiated after a flight test failure of a rocket with relatively flexible warhead that had an aluminum cylindrical shell structure with a thickness of 3 mm. Basically the same rocket, but with a much stiffer warhead made of steel with the thickness of 12 mm, has passed the flight test successfully. It has been assumed, that the failure was caused by the warhead flexibility, which affects the rocket stability margin. In addition to this reason, the possibility of failure as a result of large angle of attack within the stable condition was also considered. Such large angles of attack can cause a mechanical failure of the rocket fins. Thus, two tasks have been formulated for the rocket dynamic analysis in order to study the failure mode: a) analyze aeroelastic stability of the both flexible and stiff rockets; b) calculate angles of attack as a function of time especially during the powered phase of flight.

Aeroelastic analysis of rockets and missiles is a well developed subject that has been treated by different authors using different analytical and numerical techniques. For example, D.A. O'Keepe in [1] used discretization of a rocket model by control points and calculated influence coefficients on the basis of beam theory. The rocket mass was distributed at the control points and the lift forces were calculated at each control point according to the local angle of attack. The rocket aerodynamic model was considered as almost linear. The problem has been solved for a given flight environment, meaning that the flight speed remains constant throughout the analysis. In such an approach effects like dynamic imbalance and thrust misalignment cannot be accounted for, and the rocket response time history is not available. Loads distribution as a function of time is also unavailable in this approach.

A similar analytical approach has been used by A.R. Glasson et al. in [2]. In [3], C.P. Young, Jr. analyzed a steady state aeroelastic behavior of a spinning rocket having an aerodynamic asymmetry. The aerodynamic asymmetry has been linked to the rocket spin and stability margins were calculated. However, in these investigations neither dynamic imbalance influence nor thrust misalignment effect and response time history were available.

K.S.lee et al. in [4] applied MSC/NASTRAN transfer functions for launch vehicle air-loads analysis. This method allows to connect a thrust vector control system to the vehicle dynamic model and to analyze the system response under gusts and control forces. However, this method considers a steady state flight condition, meaning that the axial velocity remains constant and thus the aerodynamic loads are not functions of the airspeed, but only of the local angles of attack.

This article uses a nonlinear dynamic analysis method in order to simulate a rocket behavior. Time history of all solution parameters and aeroelastic analysis results are obtained with this method within a single computer run.

The loads acting on the rocket come from the following sources:

1. Aerodynamic forces and moments.
2. Loads generated by the dynamic imbalance and by thrust misalignment.
3. Gravity.
4. Thrust.

MSC/NASTRAN includes an Aeroelastic Supplement that can be used to perform aeroelastic analyses of all kinds. However, aeroelastic analyses of a rocket can also be performed using combinations of NOLIN entries. These entries are used in order to generate complicated forcing functions which are functions of some of the solution variables. This approach allows the investigation of the influence of rocket flexibility on its stability and the generation of a complete time history of rocket behavior.

The static stability of a rigid rocket is characterized by Figure 1 which shows a typical movement of a rocket center of mass and aerodynamic center as a function of time during the burning phase. Figure 1 also shows the same behavior, but for a flexible rocket. In this case the center of mass moves like in the rigid rocket, but the aerodynamic center movement becomes nonlinear, reducing the rocket's stability margin. In several cases there is a possibility that the rocket will loose its stability as a result of its flexibility. The solid line in the Figure 1 shows a typical behavior of a rigid and a stable flexible rocket, while the dashed line shows the typical behavior of an unstable flexible rocket.

The aerodynamic parameters of both rockets under consideration are identical. The aerodynamic coefficients are known from the wind tunnel tests as a function of Mach number. The center of gravity location is the same for both configurations as well as all other inertia parameters.

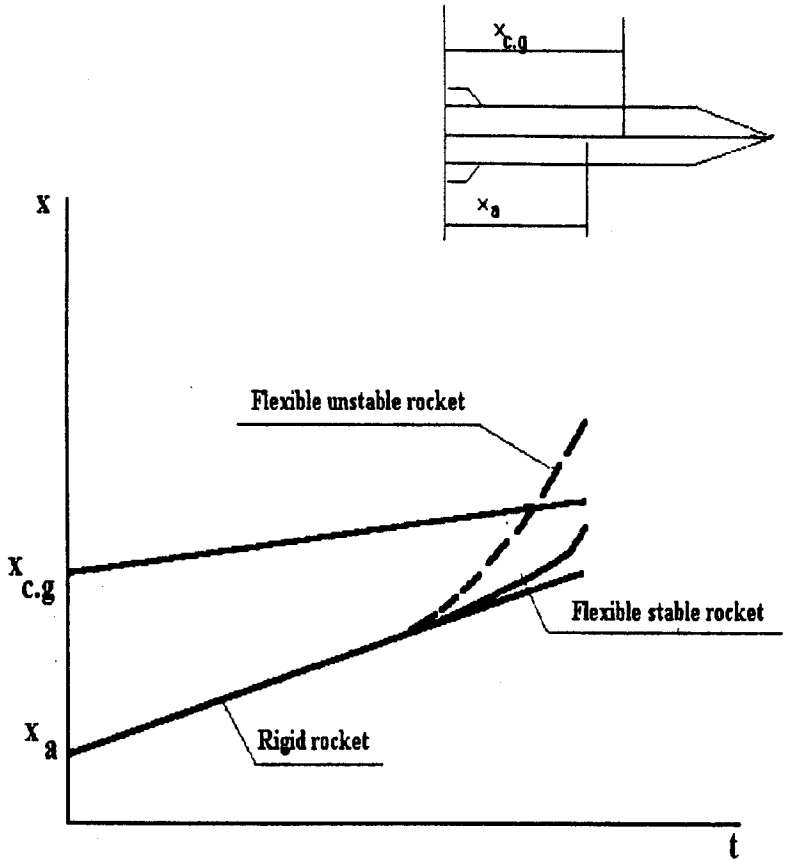

Figure 1 Center of mass and aerodynamic center shift in rigid, flexible stable and flexible unstable rockets during the burning phase.

Problem definition

The problem to solve is shown schematically in Figure 2 below.

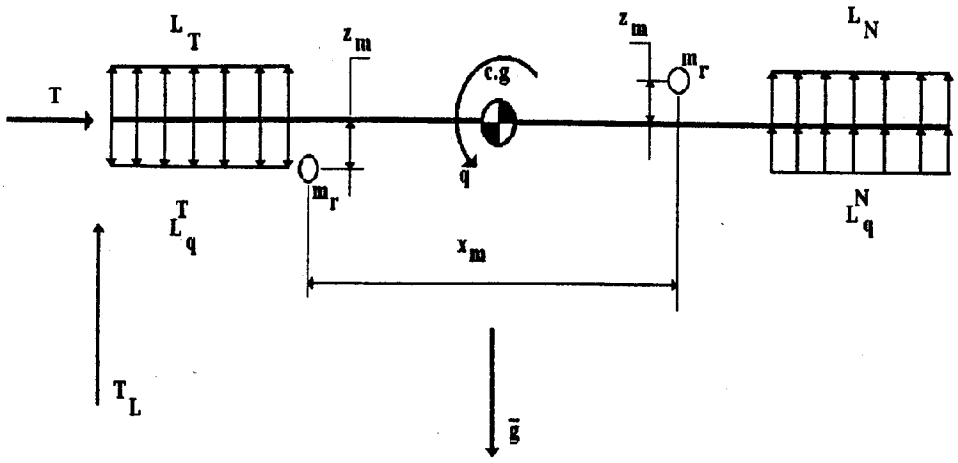

Figure 2 Rocket and rocket loads diagram.

The loads considered in the analysis are:

- Aerodynamic lift on nose and tail.
- Aerodynamic damping lift load on nose and tail.
- Thrust force.
- Gravity.
- Pitch moment created by the rocket dynamic imbalance.

The aerodynamic damping is an additional lift component caused by the rocket angular velocity.

The purposes of the analysis are:

- Calculation of the loads on the rocket elements as a function of time.
- Investigation of the rocket stability as a function of its flexibility and calculation of the rocket stability margin, including effects of thrust misalignment and dynamic imbalance.
- Calculation of the time history of the rocket response.

Several assumption have been made in the current analysis:

- The rocket mass matrix and stiffness matrix are constant throughout the entire solution. This assumption is forced by MSC/NASTRAN because in nonlinear transient analysis - SOL 99 the mass matrix cannot be updated as a function of a model distortion.
- The dependence of the aerodynamic coefficients on the Mach number has been replaced by the dependence on the velocity. This assumption is based on the fact that the burning phase duration is relatively short, and thus the speed of sound in the area under consideration can be assumed constant.
- The current investigation deals with the rocket dynamics only and thus is not connected to the rocket trajectory calculations.
- The lift force on the nose and on the tail has been equally distributed along their length. This distribution can be refined upon availability of more accurate data.
- Values of dynamic imbalance and thrust misalignment are based on some statistical parameters used in the common practice.

The loads are defined according to the following equations:

$$L_N = \frac{1}{2}\rho V^2 C_{L_\alpha}^N \alpha_N A \qquad (1)$$

$$L_T = \frac{1}{2}\rho V^2 C_{L_\alpha}^T \alpha_T A \qquad (2)$$

$$L_q^N = \frac{1}{2}\rho V^2 A \frac{q x_N}{V} C_{L_\alpha}^N \qquad (3)$$

$$L_q^T = \frac{1}{2}\rho V^2 A \frac{q x_T}{V} C_{L_\alpha}^T \qquad (4)$$

$$T = T(t) \qquad (5)$$

$$T_L = T\alpha_m \qquad (6)$$

The rocket equation of motion reads:

$$[M]\{\ddot{x}\}+[C]\{\dot{x}\}+[K]\{x\}=\{F(t,x,\dot{x})\} \qquad (7)$$

The rocket mass and stiffness matrices are directly generated from the rocket finite element model that is built of BAR elements. The damping matrix is generated using an assumption of 4% structural damping. The external loads are applied according to the eqs. (1) through (6). The gravity acceleration is applied through GRAV entry. The rolling speed and pitch moments are applied through RFORCE entry. This speed is known from flight tests as a function of time. The last two entries are applied dynamically using LSEQ entry. The thrust is applied as a prescribed function of time using the TLOAD1 entry. The aerodynamic loads are applied on the nose and the tail GRID points according to the scheme provided in Figure 3 below. The NOLINs used in the scheme cannot generate the forcing functions directly as required by the equations (1) through (4). In order to generate these forcing functions auxiliary elements are necessary. The auxiliary elements are of the ROD type; they have only one active degree of freedom and are used to convert an external load into a displacement that is equal to the load.

Lift coefficient of the nose and the tail is a function of the speed and not a function of the angles of attack for small angles. The coefficient is applied on an auxiliary ROD element as a known function of the velocity. The auxiliary ROD is used to convert a nonlinear load defined by the NOLIN1 into a displacement for further manipulations. A NOLIN2 is used to generate a multiplication of the local speed by the local angle of attack. It is applied on another auxiliary ROD element. Then the "displacements" of the RODs are multiplied using another NOLIN2 in order to generate the actual forcing function. The application of the aerodynamic damping is performed in a similar way.

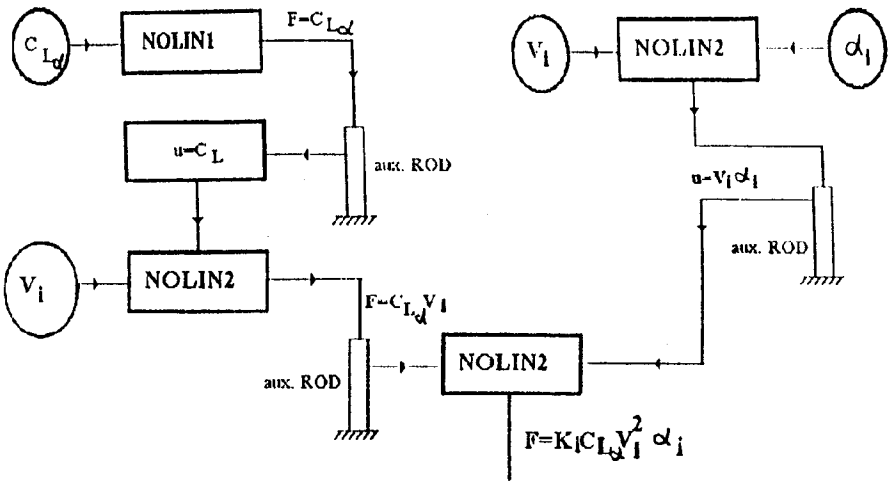

Figure 3 Nonlinear loads generation scheme for a linear aerodynamic model.

The rocket model with the auxiliary elements is shown in Figure 4 below.

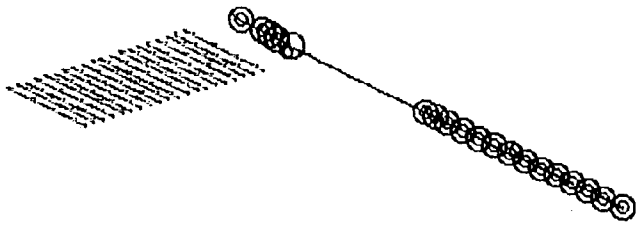

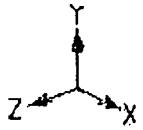

Figure 4 Rocket model with auxiliary elements.

Analysis results

Rocket with steel warhead.

Figure 5 shows the time history of the angle of attack of GRID point no. 1 - nose and GRID point no. 32 - tail. The graph demonstrates that there is no visible difference between the two curves. Figure 6 shows the bending distortion of the rocket at the time of 2.2 sec when the maximum speed is achieved. The maximum linear distortion is 31.37 mm, measured between the nose and the rocket center of mass. The maximum angle of attack is about 1.5 degree. Such an angle of attack cannot cause any structural problem to the rocket fins or their attachments and does not require an application of a nonlinear aerodynamic model. Figure 7 shows the bending moment distribution along the rocket axis at the time instant of 2.2 sec. The maximum bending moment is about 1200 NM at the middle of the rocket.

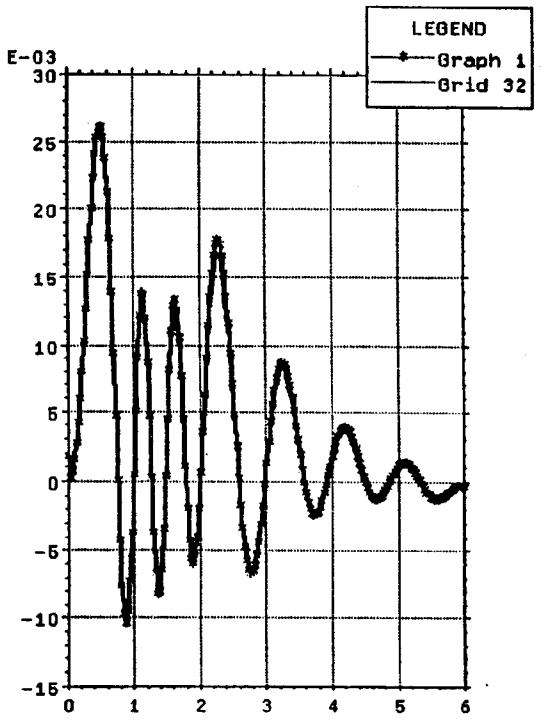

Figure 5 Angle of attack of the steel warhead rocket vs. time

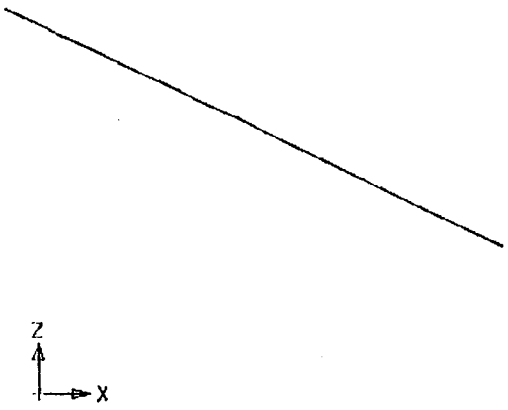

Figure 6 Deformed shape of the steel warhead rocket

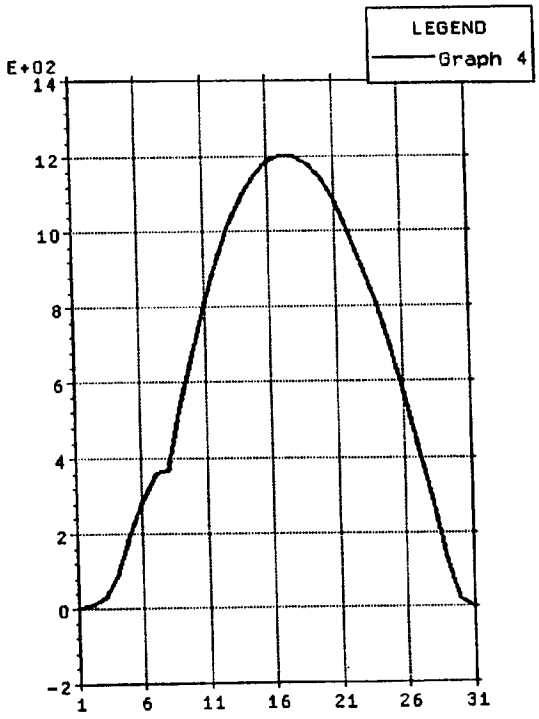

Figure 7 Bending moment distribution in the steel warhead rocket.

Rocket with aluminum warhead

Figure 8 shows the time history of the angle of attack of GRID point no. 1 - nose and GRID point no. 32 - tail. From this figure one can see that the rocket begins to develop large angles of attack immediately after the burnout, when the maximum speed is achieved. Figure 9 shows the same graph focusing the attention on first 2.3 sec of flight. The maximum angle of attack within the stable phase does not exceed 1.5 degree, meaning that the failure was caused by the loss of stability. Bending deformation of the rocket is much more visible - see Figure 10 that shows the deformed and undeformed shapes of the rocket at the time instant of 2.2 sec. The bending deformation in this case is 80.69 mm measured again as a difference between the nose linear distortion and the middle of the rocket distortion. The bending moment distribution presented in Figure 11 shows the maximum bending moment of 4600 Nm - almost four times higher than in the case of the stiff rocket at the same time instant of 2.2 sec.

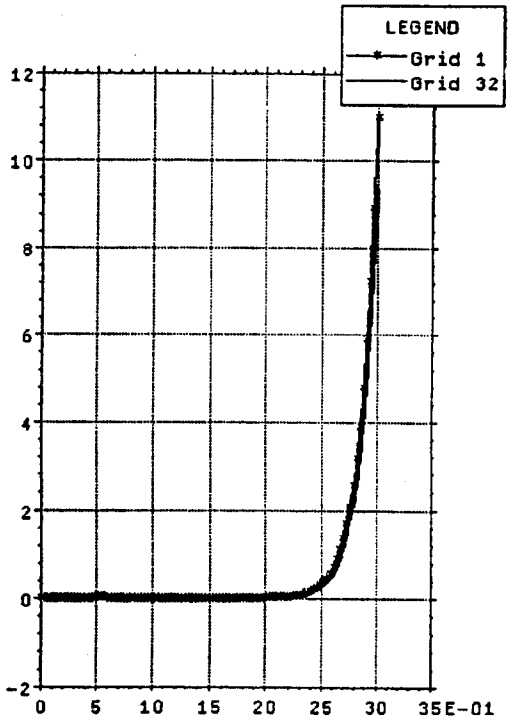

Figure 8 Angle of attack of the aluminum warhead rocket vs. time

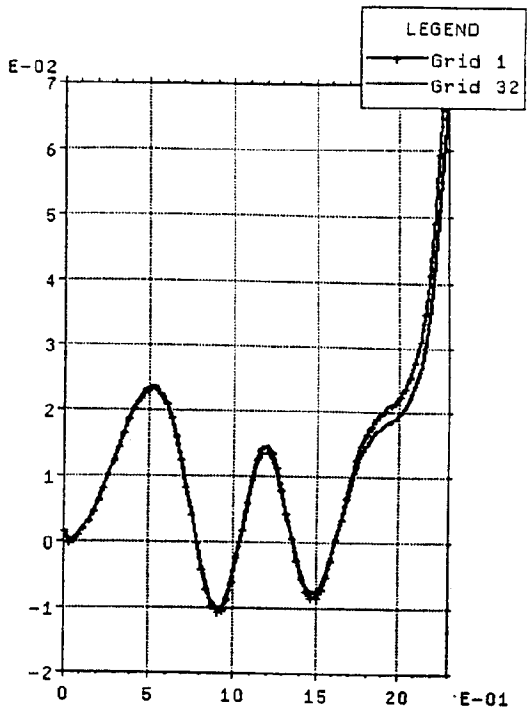

Figure 9 Angle of attack of the aluminum warhead rocket vs. time (zoom of the Figure 8)

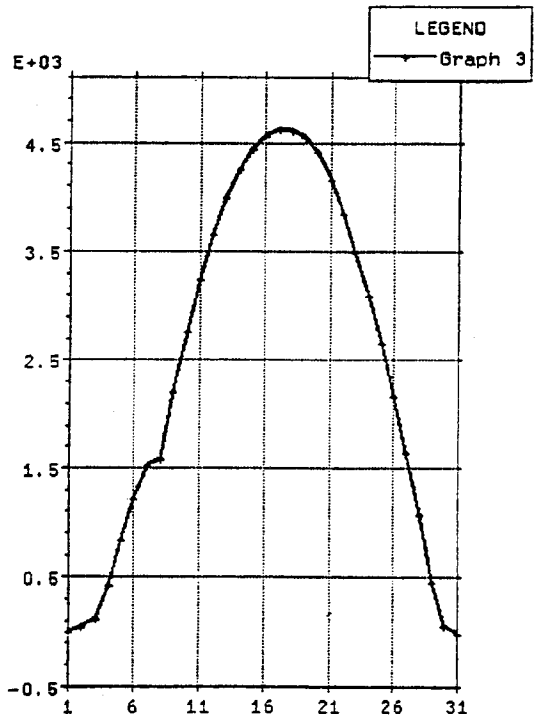

Figure 10 Bending moment distribution of the aluminum warhead rocket.

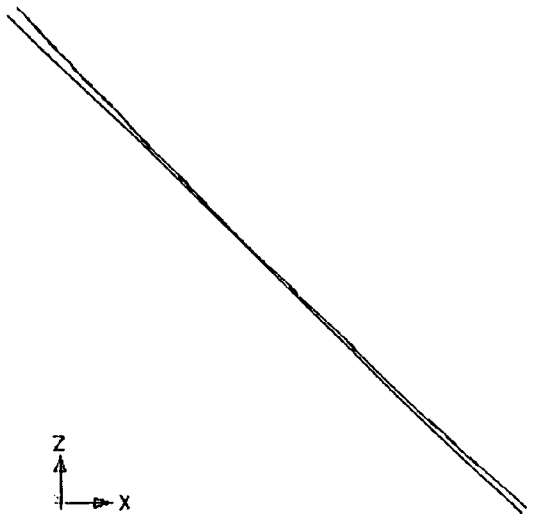

Figure 11 Deformed and undeformed shapes of the aluminum warhead rocket.

Discussion

The rocket with the steel warhead shows the behavior typical to an almost rigid rockets. The rocket with aluminum warhead shows the behavior typical to a condition of a loss of stability as a result of the warhead flexibility. Bending moment grows by almost a factor of four as a result of larger angle of attack and bending of the rocket becomes clearer. However, both rockets behave identically when the velocities are relatively low.

Figure 8 shows the development of the large angles of attack as a function of time, meaning that the rocket becomes unstable. This kind of behavior is similar to the one obtained while analyzing a case of bifurcation of equilibrium by the method of large displacements - see for example [5]. As in the case of bifurcation, it is necessary to introduce a small imperfection into the system in order to initiate the process. Like in the case of static stability, also here the external load is gradually increased as a function of time and under curtain "critical" load, the system starts to develop large deflection. However, in the rocket dynamics case, there is no need to do any iteration compared to the static stability case.

Conclusions

1. MSC/NASTRAN has been found as analytical tool that is capable to perform nonlinear dynamic analysis with forcing function that have a high degree of non linearity through the use of NOLINs combinations.

2. It is possible to analyze simultaneously a complete time history of a free flight rocket response and the stability of that rocket as an inherent part of the analytical procedure.

3. Introduction of small imperfection is necessary in the solution procedure described herein, similarly to an elastic system stability analysis, while analyzing it by the method of large displacements. As a small imperfection one can use dynamic imbalance, thrust misalignment, or a combination of both of these.

4. In the present version of MSC/NASTRAN, the movement of the center of mass location could not be modeled because there is no option to remove elements from the model during the solution phase. Implementation of such feature can be of possible improvements in the future.

Acknowledgments

This research was initiated and supported by TAAS - Israel Industries Ltd in most of its parts.

References

1. David A. O'Keepe , **General Static Aeroelastic Analysis of a Body of Revolution**, AIAA journal, December 1965.

2. A.R.Glasson and K.G.Pearson, **A FORTRAN Computer Program for Steady State Aeroelastic Evaluation of Slender Nonrolling Rocket Vehicles**, Australian Defense Scientific Service, Techical Note HSA 128, October 1967.

3. Clarence P.Young, **On the Steady State Aeroelastic Behavior of a Spinning Rocket Having Aerodynamic Asymmetry**, AIAA Second Sounding Rocket Conference, Williamsburg, Virginia, December 1970.

4. Kuan S.Lee, R.P.Miller and T.W.Porada, **An Application of MSC/NASTRAN Transfer Functions for Launch Vehicle Air-Loads Analysis**, 1991 MSC World Users' Conference.

5. M.A.Mikulinsky and D.S.Livshits, **Pre- and Post-Buckling Analysis of Simple Systems**, presented at the Seventh World Congress on Finite Element Methods, Monte Carlo, 1993.

6. **MSC/NASTRAN Handbook for Dynamic Analysis.**